

The Effect of Chlorine Treatment on the Dispersion of Platinum Metal Particles Supported on Silica and γ -Alumina

K. FOGER AND H. JAEGER

*CSIRO Division of Materials Science, Catalysis and Surface Science Laboratory,
University of Melbourne, Parkville, 3052, Victoria, Australia*

Received December 21, 1983; revised October 2, 1984

The reaction of Pt metal particles on SiO_2 (Aerosil) and $\gamma\text{-Al}_2\text{O}_3$ supports with Cl_2 (0.2–100% by vol.) in N_2 or He in a flow system at temperatures (T_r) in the range 320–700 K has been studied with XRD, TEM, uv-diffuse reflectance spectroscopy, and temperature-programmed reduction (TPR) of the products. On SiO_2 , for 5–25% Cl_2 only PtCl_2 results, forming large (up to 500 nm diam.) single-crystal sheets for $500 < T_r \leq 700$ K and increasingly fine grained to amorphous aggregates for $500 > T_r \geq 320$ K. For 25–100% Cl_2 various products form depending on T_r : (i) $320 \leq T_r < 520$ K a Pt(IV) chloride/support-surface complex $[\text{Pt(IV)Cl}_x]$; (ii) $520 \leq T_r < 590$ K PtCl_4 (needles); (iii) $590 \leq T_r < 670$ K PtCl_3 (needles); and (iv) $670 \leq T_r \leq 700$ K PtCl_2 (chunky). For $T_r \geq 600$ K Pt is increasingly lost from the support for any concentration of Cl_2 . On $\gamma\text{-Al}_2\text{O}_3$, only support-surface bound $[\text{Pt(IV)Cl}_x]$ is formed and no Pt is lost from the support for $T_r \leq 700$ K. On both supports, Pt metal is redispersed—its mean particle size is decreased on Cl_2 treatment followed by reduction—only if $[\text{Pt(IV)Cl}_x]$ is formed. Physically distinct chlorides, crystalline or amorphous, always reduce to low surface area aggregates. © 1985 Academic Press, Inc.

INTRODUCTION

Supported noble metal catalysts are widely used for the processing of hydrocarbons. During operation, the activity of such catalysts slowly decreases due to the deposition of carbon and feedstock impurities or the agglomeration of the metal particles. To regenerate catalysts, the deposits are first removed by heating in oxidizing atmospheres. This may lead to further agglomeration of the metal and, in some alloy catalysts, may change the surface composition of metal particles or cause phase separation. Treatments with halogen compounds are most commonly employed to redisperse and realloy noble metal particles and numerous patents have been published (1), but few studies have appeared in generally accessible journals (2, 3, 14). One of those (14) dealt in some detail with the effects of treatment gas mixtures such as Cl_2 /inert gas or Cl_2 /air on $\text{Pt/Al}_2\text{O}_3$ catalysts, but the study lacks direct evidence for the nature of platinum halides formed during the treat-

ment. We therefore decided to study the redispersion of supported platinum catalysts by halogen treatment utilizing a combination of techniques—X-ray diffraction (XRD), transmission electron microscopy (TEM), uv-diffuse reflectance spectroscopy, and temperature-programmed reduction (TPR)—which would allow us to observe directly the extent of chlorination, the nature and morphology of the formed halides, and the dispersion of the metal after reduction treatment. Three model Pt catalysts, one supported on silica ($d_m \sim 9$ nm) and two supported on $\gamma\text{-Al}_2\text{O}_3$ ($d_m = 50\text{--}500$ and ~ 3 nm) were exposed at atmospheric pressure to a variety of Cl_2/N_2 mixtures at selected temperatures in the range 320 to 700 K and examined at various stages of treatment by above-listed techniques.

EXPERIMENTAL

Materials

The dispersion of the following systems was studied:

(a) *1.5% Pt on SiO_2* . Aerosil 200 (Degussa) impregnated to incipient wetness with H_2PtCl_6 was dried in air at 300 K, reduced in H_2 for 15 h at 670 K, then sintered in O_2 for 3–5 h at 900 K and finally reduced in H_2 at 670 K for 15 h. The resulting Pt particles had a wide size distribution with a mean diameter, $d_m \approx 9$ nm.

(b) *2.5% Pt on $\gamma\text{-Al}_2\text{O}_3$* . PtCl_2 particles were mixed with the support (Akzo-Chemie, 125 m^2/g) and reduced in H_2 for 15 h at 670 K to produce metal particles with diameters, d_m , in the range 50–500 nm.

(c) *2.0% Pt on $\gamma\text{-Al}_2\text{O}_3$* . was prepared by impregnating $\gamma\text{-Al}_2\text{O}_3$ (Akzo-Chemie, 125 m^2/g) with H_2PtCl_6 followed by drying at 300 K and reduction in flowing H_2 at 670 K for 15 h. Metal particles with a mean diameter of 3 nm were present.

(d) *Mixtures of 5% PtCl_2 particles ($d_m \geq 50$ nm) and $\gamma\text{-Al}_2\text{O}_3$ or SiO_2* . These mixtures were prepared by dry ball milling of the components.

Procedures

A stream of Cl_2 (5–100% by vol.) in N_2 was passed through 0.1 to 0.2 g of model catalyst or PtCl_2 –support mixture placed loosely in a vertical 8-mm-diam. silica tube reactor. The reactor was then heated at a selected temperature in the range 320 to 700 K for a predetermined time, allowed to cool to room temperature, and purged with pure N_2 . For 25% Cl_2 or less the flow rate of the gas mixture was 20 cm^3/min but for higher Cl_2 concentrations it was 10 cm^3/min . Some experiments were carried out with reactive gas streams consisting of Cl_2 (up to 10 vol%) in 1% O_2 in He or in air.

The uv-diffuse reflectance of chloride compounds on the support was measured with a Pye SP 100 uv-vis instrument using the pure support as a reference and plotting the spectra obtained over the range 300 to 800 nm in the form of the second derivative. Minima were assigned to certain Pt chloride compounds on the basis of comparison with traces for PtCl_2 mixed with SiO_2 or $\gamma\text{-Al}_2\text{O}_3$ and for H_2PtCl_6 impregnated on the sup-

ports. PtCl_2 gave rise to somewhat broad minima at 515 and 375 nm, while H_2PtCl_6 produced sharper minima at 435 and 355 nm (e.g., see traces 5 and 6 in Fig. 4). The X-ray data were obtained with a vertical D 500 diffractometer on a K 805 generator (Siemens A.G.) using Ni-filtered $\text{CuK}\alpha_{1,2}$ or monochromated $\text{CuK}\alpha_1$ radiation. Electron microscopy was carried out at 100 kV in a JEM 100 CX fitted with a special high-resolution objective pole piece and top entry tilting facility. The apparatus and procedure for obtaining TPR profiles have been described earlier (4). TPR experiments were performed on 0.15 g Pt/SiO_2 and 0.1 g of $\text{Pt}/\text{Al}_2\text{O}_3$ samples; 3% H_2 in N_2 was used as a reduction mixture and the temperature was increased at a rate of 10 K min^{-1} .

RESULTS

Cl_2 Treatment

On both supports Pt particles were readily attacked by Cl_2 over the whole temperature range. For example, for 1.5% Pt ($d_m \approx 9$ nm) on SiO_2 , the bluish grey color typical of the metal disappeared and metal particles could no longer be detected on the support with XRD and TEM after heating in streams of 10% Cl_2 in N_2 at temperatures T_r of 570, 470, 370, and 320 K for 0.5, 2, 4, and 12 h, respectively. In the alumina-supported catalysts—2% $\text{Pt}/\text{Al}_2\text{O}_3$ ($d_m \approx 3$ nm) and 2.5% $\text{Pt}/\text{Al}_2\text{O}_3$ ($d_m = 50$ to 500 nm)—the metal was completely converted to the halide in 2.5 h and in 4 h by treatment in flowing 10% Cl_2 in N_2 at T_r of 470 K. Taking into account the different metal loadings and particle sizes of the three model catalysts, the rates of chloride formation appeared to be very similar, but the nature, distribution, and morphology of the reaction products depended on the substrate and chlorine concentration (see Table I).

Pt on SiO_2 Treated in 5–10% Cl_2

$470 \leq T_r \leq 670$ K. When the catalysts were treated in this range with $\leq 10\%$ Cl_2 metal peaks in XRD traces disappeared and

TABLE I

| Catalyst treatment | | Chloride phases detected with | | | TPR | | d_{Pt}^a (nm) after TPR | Remarks |
|--|----------|---|---|----------------------|---|----------------------|---|--|
| T_r (K) | Time (h) | TEM and/or XRD | Ultraviolet diffuse reflectance spectroscopy | T_{max} (K) | moles $\text{H}_2 \times 10^5 \frac{\text{g}}{\text{g}_{\text{cat}}}$ | T_{max} (K) | moles $\text{H}_2 \times 10^5 \frac{\text{g}}{\text{g}_{\text{cat}}}$ | |
| 1.5% Pt/SiO ₂ | | | | | | | | |
| 320 | 12.0 | Amorphous Pt(II) chloride Amorphous Pt(II) chloride + PtCl ₂ ^b PtCl ₂ ^b | Mainly Pt(II) chloride and some [Pt(IV)Cl ₂] _s | 310 | 6.8 | — | — | d_{Pt} of starting material before Cl ₂ treatment and TPR |
| 420 | 3.5 | | | 350 | 2.8 | 480 | 9.2 | Bimodal particle size Distributions $d_{\text{Pt}} \geq 10$ nm ≤ 2 nm |
| 470 | 2.0 | | | 320, 350 | 5.9 | 470 | 3.5 | |
| 570 | 0.5 | | | 360 | 6.1 | 470 | 2.2 | |
| 470 | 2.0 | None PtCl ₄ ^b PtCl ₃ ^b | [Pt(IV)Cl ₂] _s — — | — | — | 500 | 15.0 | Loss of Pt as PtCl ₂ |
| 570 | 0.5 | | | — | — | 500 | 13.0 | |
| 620 | 0.5 | | | 370 | 4.8 | 500 | 1.6 | |
| 2.2.5% Pt/Al ₂ O ₃ | | | | | | | | |
| 470–670 | 4–0.5 | None None None | [Pt(IV)Cl ₂] _s [Pt(IV)Cl ₂] _s [Pt(IV)Cl ₂] _s | — | — | 500 | 25.0 | Residual Pt particles observed by TEM and XRD after chlorine treatment |
| 470 | 2.0 | | | 280 | 0.6 | 500 | 10.0 | |
| 520 | 1.0 | | | — | — | 500 | 19.0 | |
| 2.0% Pt/Al ₂ O ₃ | | | | | | | | |
| 470 | 2.5 | None | [Pt(IV)Cl ₂] _s | — | — | 500 | 21.0 | d_{Pt} of starting material before Cl ₂ treatment and TPR |
| PtCl ₂ + Al ₂ O ₃ | | None | [Pt(IV)Cl ₂] _s | 320 | — | 500 | — | 50–500 |
| 520–670 | 0.5 | | | — | — | 500 | 36.0 | |

^a Measured with TEM or XRD.^b PtCl₂, PtCl₃, PtCl₄ represent crystalline phases.

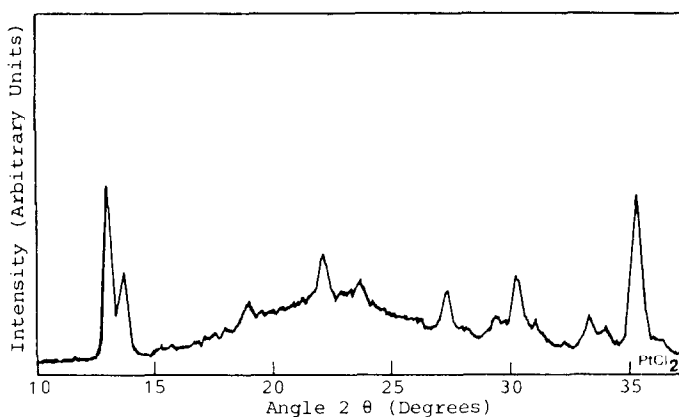


FIG. 1. XRD trace of Pt/SiO_2 treated with 10% Cl_2 in N_2 at $470 \leq T_r \leq 670$ K. The peaks match the reported XRD profile of PtCl_2 .

new peaks, which could all be assigned to PtCl_2 (5) became prominent (Fig. 1). These changes were supported by TEM observations where images of metal particles on the support disappeared and it became possible to detect large isolated particles which sometimes exceeded the largest observed metal particles by about 10^3 times. Selected area diffraction (Fig. 2a) revealed that such particles were either single crystals of PtCl_2 or consisted at most of only a few grains of this material; but the compound decomposed in the electron beam and within a few minutes of observation, the spot patterns of PtCl_2 faded to be replaced by stable diffuse Pt metal ring patterns (Fig. 2b). Examination of images showed that the ring patterns resulted from Pt crystal aggregates whose sizes, shapes, and distributions reflected those of the initial PtCl_2 particles. At the high end of the temperature range the PtCl_2 particles had distinct crystallographic shapes (Fig. 3a) but as T_r was lowered the shapes became irregular (Fig. 3b). Evaluation of uv-diffuse reflectance spectra suggested that treatment at $T_r \leq 570$ K produced mainly PtCl_2 but that appreciable concentrations of Pt(IV) chloride¹ were produced, besides PtCl_2 , toward the lower

end of this range of T_r (e.g., compare traces 3 and 4 with 5 and 6, Fig. 4).

When T_r was kept below 570 K no appreciable loss of Pt from the catalyst was observed if the Cl_2 treatment was terminated soon after the color of the sample changed from bluish grey to creamy yellow, but as T_r was raised above 570 K increasing concentrations of PtCl_2 were detected in cold parts of tubing downstream from the catalyst before all the Pt had reacted and treatment at 670 K for 2 h, for example, resulted in complete loss of Pt from the support.

$320 \leq T_r < 470$ K. In this range Pt metal peaks in XRD traces disappear but no new peaks could be detected. TEM observations showed that the disappearance of the metal was accompanied by the formation of thin sheet-like deposits, which again decomposed in the electron beam, into tenuous aggregates of small Pt particles without appreciable change in the overall outline. For $T_r > 370$ K the resulting Pt aggregates often still had regular outlines (Fig. 3c) but when T_r was below 370 K only irregular web-like nets of Pt particles were detected within the support (Fig. 3d). Visual examination showed that electron diffraction from particles with regular outlines produced initially PtCl_2 spot patterns, but the patterns changed into diffuse Pt rings before they could be recorded. Only diffuse Pt

¹ This mode to designate the nature of the chloride is used whenever the structure could not be determined.

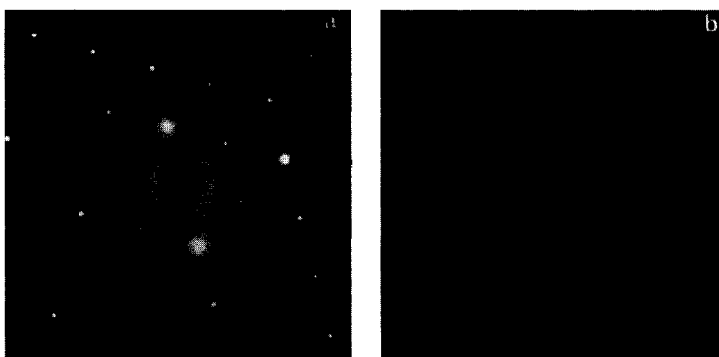


FIG. 2. Electron diffraction pattern of a PtCl₂ crystal. (a) Initial and (b) after a few minutes in electron beam.

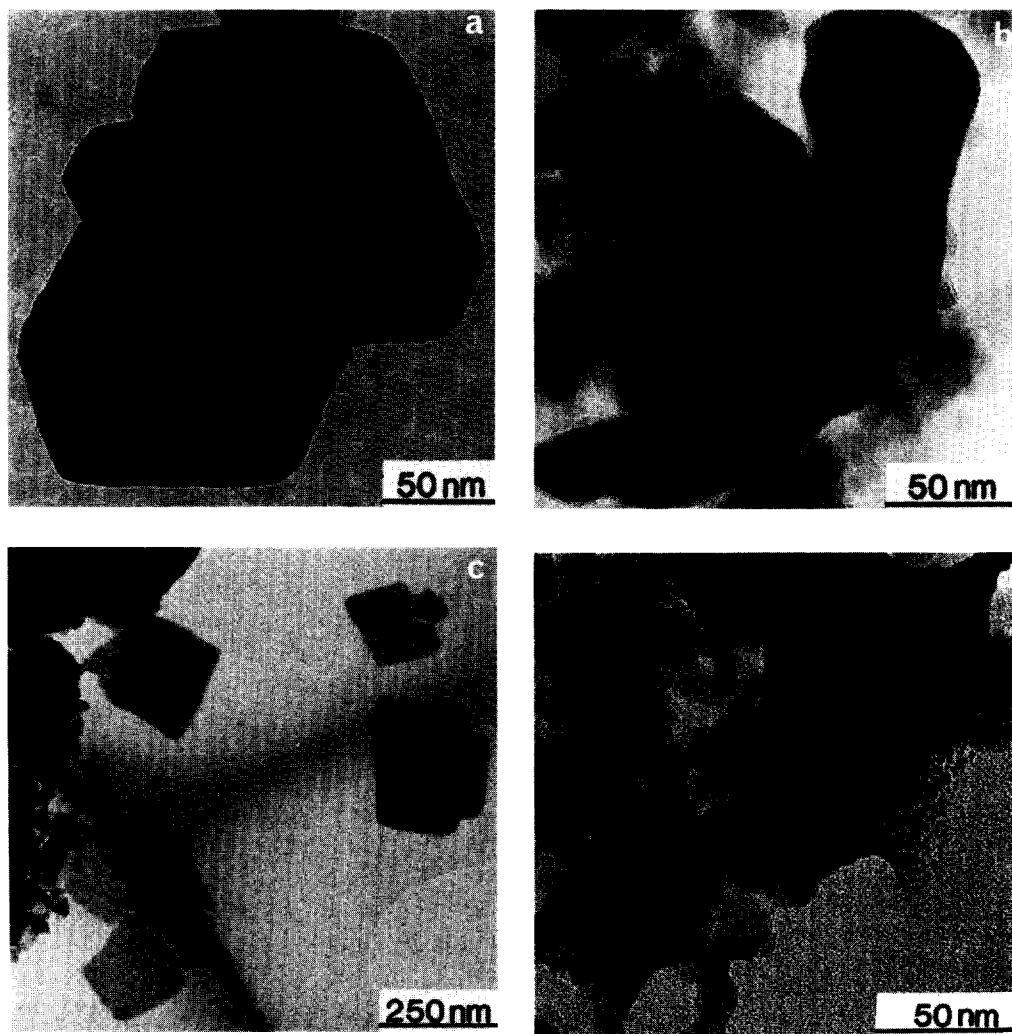


FIG. 3. Electron micrographs of platinum chlorides formed on SiO₂ in 10% Cl₂ in N₂ at (a) $T_r > 570$ K, (b) $470 < T_r < 570$ K, (c) $370 < T_r < 470$ K, (d) $T_r < 370$ K.

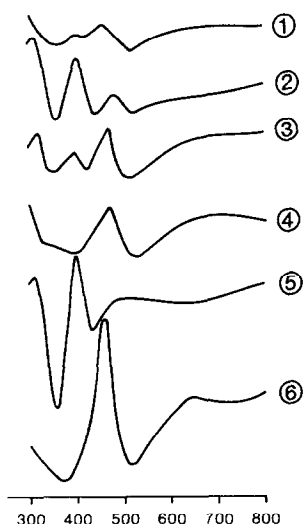


FIG. 4. Ultraviolet-diffuse reflectance spectra of Pt/SiO₂ treated in 10% Cl₂ in N₂ at $T_r = 320$ K for 12 h, 1; $T_r = 420$ K for 3 h, 2; $T_r = 470$ K for 2 h, 3; $T_r = 570$ K for 1 h, 4; H₂PtCl₆/SiO₂, 5; PtCl₂ + SiO₂ (physical mixture), 6.

ring patterns could be obtained with electron diffraction from any of the irregularly shaped material formed below 370 K. From uv-diffuse reflectance traces it was concluded that both Pt(II) and Pt(IV) chlorides were present at $T_r > 370$ K, and that the proportion of the latter increased with T_r (compare traces 1 and 2 with 5 and 6, Fig. 4), but only Pt(II) chloride could be detected with this method at $T_r < 370$ K.

Over the whole range, $320 \leq T_r \leq 590$ K, lowering the Cl₂ concentration from 10 to 5% had no appreciable effect apart from slowing down the rate of reaction and generally lowering the concentration of Pt(IV) chloride relative to that of PtCl₂ in the reaction products.

Pt on SiO₂ Treated in 25–100% Cl₂

$420 \leq T_r < 520$ K. When catalysts were treated in this range with more than 25% of Cl₂ in the gas stream, the bluish grey color, which indicated the presence of metallic Pt, faded away completely in about 3 h at 420 K and in 1 h at 520 K and with TEM or XRD neither metal particles nor any metal chloride could be detected on the substrate

after such treatment. However, uv-diffuse reflectance spectroscopy (e.g., trace 4, Fig. 5) revealed on the support Pt(IV) chloride in concentrations which corresponded to the original metal loading.

$520 < T_r \leq 590$ K. In this range the color of the catalysts changed to reddish brown and in TEM micrographs metal particles had disappeared from the substrate and instead mainly large particles (0.1–0.5 μm in size) were prominent. The latter tended to form sheets with regular outlines, but occasionally also short rods with straight sides and round ends or irregular clumps. The rods were always single crystals, the regular sheets were single crystals or consisted at most of a few largish grains, but the irregular clumps were always collections of randomly oriented small crystals. Electron diffraction indicated that the particles consisted of PtCl₄, but again the material was unstable in the beam and the patterns were quickly replaced by diffuse Pt rings and in TEM micrographs only Pt aggregates outlining the original shapes of the particles could be recorded. That the reaction product was PtCl₄ was verified from XRD traces (trace 1, Fig. 6) but care had to be taken to avoid exposing samples to the air as PtCl₄ is very deliquescent (6). Ultraviolet-diffuse reflectance spectroscopy (trace 3, Fig. 5)

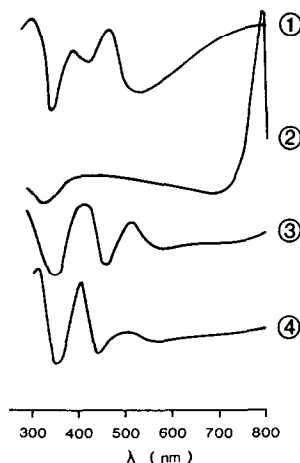


FIG. 5. Ultraviolet-diffuse reflectance spectra of Pt/SiO₂ treated in >25% Cl₂ in N₂ at $T_r = 670$ K, 1; $T_r = 620$ K, 2; $T_r = 570$ K, 3; $T_r = 470$ K, 4.

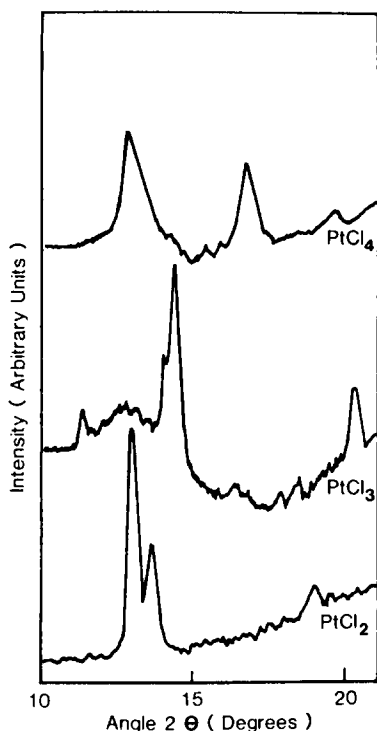


FIG. 6. XRD traces of Pt/SiO₂ treated in >25% Cl₂ in N₂ at $T_r = 570$ K (top), $T_r = 620$ K (center), and $T_r = 670$ K (bottom). The peaks match reported XRD patterns for PtCl₄, PtCl₃, and PtCl₂.

further confirmed the presence of a Pt(IV) chloride. In this temperature range small amounts of Pt were lost from the support and redeposited as PtCl₂ downstream from the samples.

$590 < T_r < 670$ K. Treatment in this region changed the color of the catalyst to bluish black and led to more obvious loss of Pt as evidenced by the formation of PtCl₂ downstream from the specimens. TEM revealed that instead of Pt particles large oblong prisms (Fig. 7) with flat or slightly rounded ends and generally round or hexagonal cross sections could be seen among the support. The prisms occurred sometimes singly (Figs. 7a and b) but more often they were present as intersecting pairs or bunches (Fig. 7c). Electron diffraction showed that individual prisms were single crystals and exhibited spacings consistent with those reported for PtCl₃ (5). That the

crystalline products in this range were exclusively PtCl₃ was confirmed with XRD (middle trace, Fig. 6) and uv-diffuse reflectance spectroscopy showed that neither Pt(II) chloride nor Pt(IV) chloride were present to any noticeable extent (e.g., see trace 2, Fig. 5). Prolonged air exposure led to the decomposition of PtCl₃ (Fig. 7d) into PtCl₂, identified by XRD, and noncrystalline Pt(IV) chloride, identified by diffuse reflectance spectroscopy.

$670 \text{ K} < T_r$. When the temperature was raised above 670 K the color of the catalyst turned initially to green and then faded as the loss of Pt became extensive and large (0.5–1 μm size) PtCl₂ crystals were deposited downstream from the specimen. Both TEM and XRD showed that large sheets of PtCl₂ were formed initially on the support, and uv-diffuse reflectance traces revealed mostly Pt(II) chloride besides small amounts of Pt(IV) chloride (see trace 1, Fig. 5).

Pt on γ -Al₂O₃ Treated in 0.2–100% Cl₂

$320 < T_r < 700$ K. TEM and XRD showed that over the whole range of temperatures and Cl₂ concentrations Pt particles disappeared from the support at rates which were similar to those observed for the same conditions with Pt on silica, e.g., no metal particles could be detected in 2.5% Pt/Al₂O₃ ($d_m = 50$ to 500 nm) after treatment in 10% Cl₂ in N₂ mixtures at 470 K for 4 h and in 2% Pt/Al₂O₃ catalysts ($d_m \approx 3$ nm) after 2.5 h, but contrary to observations in silica supported catalysts no platinum chloride phases could be detected with these techniques either on the support or in the tubes leading from the reactor. However, uv-diffuse reflectance spectroscopy revealed that chlorine treatment did always lead to the formation of Pt(IV) chloride on the substrate (e.g., compare traces 3, 4, and 5 with 1 and 2, Fig. 8).

Mixtures of PtCl₂ and SiO₂ or γ -Al₂O₃ Treated with 10% Cl₂

$320 < T_r \leq 670$ K. For PtCl₂/SiO₂ mix-

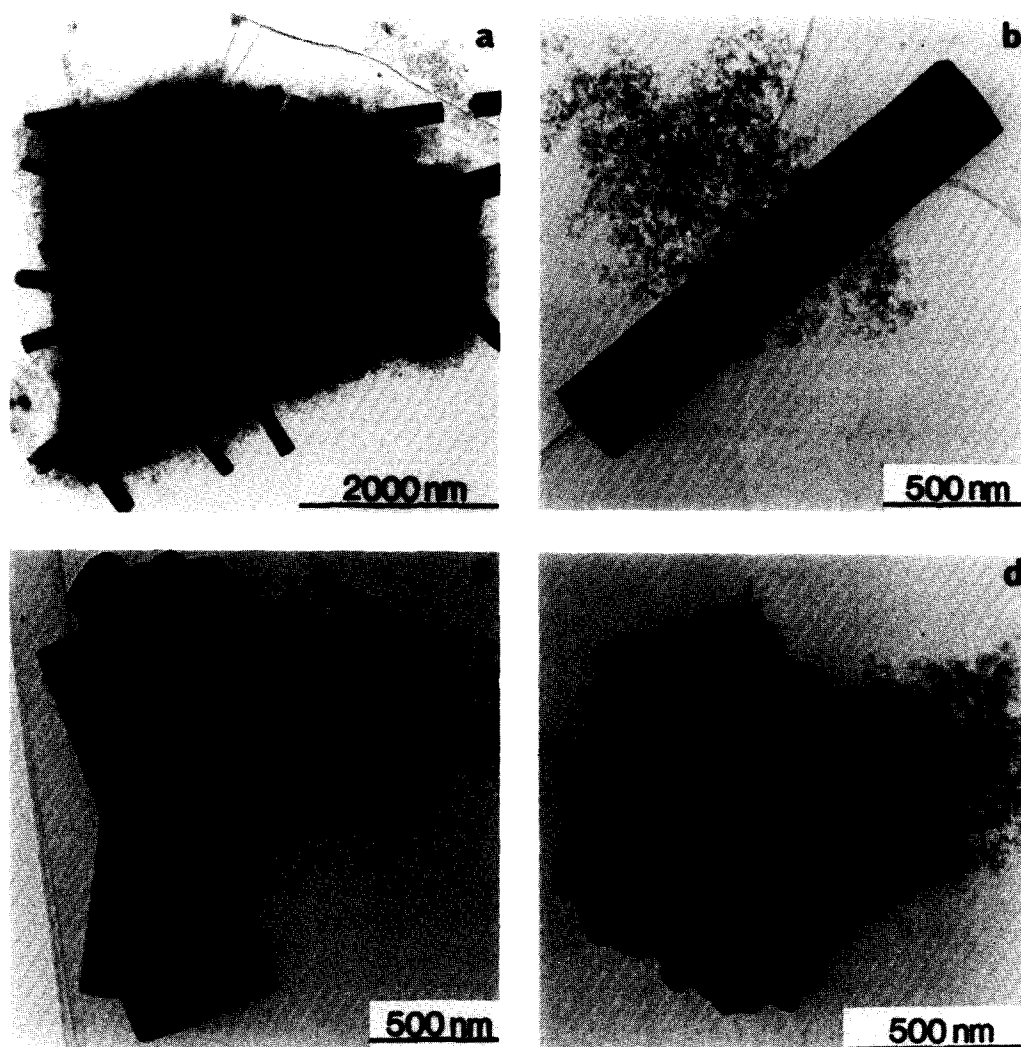


FIG. 7. Transmission electron micrographs of PtCl_3 particles formed in $>25\%$ Cl_2 in N_2 streams in the temperature range $590 < T_r < 670$ K, immediate after reaction (a, b, c), and after 2 days storage (d).

tures the only changes observed with XRD, TEM, and uv-diffuse reflectance spectroscopy were extensive losses of PtCl_2 from the reactor for $T_r > 520$ K.

For $\text{PtCl}_2/\gamma\text{-Al}_2\text{O}_3$ mixtures XRD and TEM revealed that PtCl_2 particles disappeared readily from the mixture at $T_r > 520$ K but no formation of a new phase could be detected either on the $\gamma\text{-Al}_2\text{O}_3$ or in the tubing from the reactor at any temperature in this range. However, uv-diffuse reflectance spectroscopy showed that Pt(IV) chloride was formed on the $\gamma\text{-Al}_2\text{O}_3$. The conversion

of PtCl_2 to Pt(IV) chloride was complete after about 0.5 h at $T_r \approx 520$ K.

Reduction of Pt Chlorides

(a) *TPR profiles: $\text{Pt}/\gamma\text{-Al}_2\text{O}_3$.* A single maximum at 500 K was observed when $\text{Pt}/\gamma\text{-Al}_2\text{O}_3$, treated in gas streams containing 0.2–100% Cl_2 in the temperature range $320 < T_r < 770$ K, was subjected to TPR (e.g., trace ---, Fig. 9). Similar TPR maxima resulted for $\text{PtCl}_2/\gamma\text{-Al}_2\text{O}_3$ mixtures, which had been treated in 10% Cl_2 at $T_r = 673$ K (trace ■, Fig. 10), while $\text{PtCl}_2/\gamma\text{-Al}_2\text{O}_3$ mix-

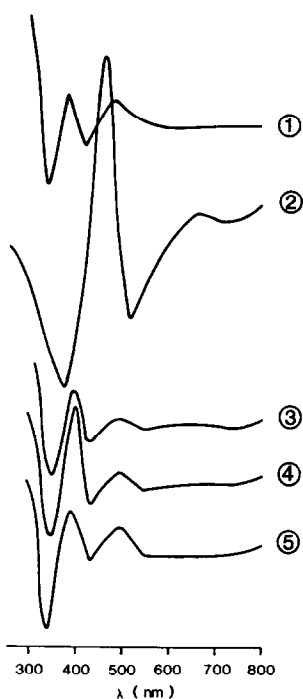


FIG. 8. Ultraviolet-diffuse reflectance spectra of $\text{H}_2\text{PtCl}_6/\text{Al}_2\text{O}_3$, 1; $\text{PtCl}_2 + \text{Al}_2\text{O}_3$, 2; $\text{Pt}/\text{Al}_2\text{O}_3$ treated in 0.2–100% Cl_2 in N_2 at $T_r = 470$ K, 3; $T_r = 570$ K, 4; $T_r = 670$ K, 5.

tures before Cl_2 treatment resulted in a sharp TPR maxima at 320 K (trace ●, Fig. 10).

Pt/SiO₂. For platinum on SiO_2 treated at different T_r in various Cl_2 concentrations, a variety of TPR peaks were observed. For example, treatment in 10% Cl_2 at $T_r \approx 320$ K resulted in a single TPR maxima at 310 K (trace ■, Fig. 9). When T_r was increased to 420 K, two broad maximum appeared, a small one at 350 K and a main one at 480 K (trace ▲, Fig. 9). For $T_r \approx 470$ K, TPR traces showed two narrow main maxima at 320 and 350 K and a small broad peak at 470 K (trace ●, Fig. 9). Increasing T_r further to 570 K resulted in a sharp TPR peak at 360 K with a shoulder at 470 K (trace ◆, Fig. 9). A similar maximum appeared when PtCl_2 mixed with SiO_2 was subjected to TPR (trace ◆, Fig. 10).

TPR profiles of Pt/SiO_2 catalysts treated in gas streams containing more than 25%

chlorine are shown in Fig. 11. When T_r was 470 K a single maximum at 500 K appeared (trace ▲, Fig. 11). A similar peak was observed when T_r was in the range $520 < T_r < 590$ K (trace ●, Fig. 11). Pt/SiO_2 treated in >25% Cl_2 between 590 and 670 K gave rise to two TPR maxima, one at 370 K and the other at 500 K (trace ■, Fig. 11). When T_r was increased further a single TPR peak at 360 K was observed. Quantitative data extracted from TPR profiles are summarized in Table I together with information about the structure and composition of the chloride and average sizes of platinum metal particles observed after TPR.

(b) *Structural changes: Pt/ γ -Al₂O₃.* When the Pt had been completely reacted with Cl_2 over the whole range of T_r and Cl_2 concentrations, reduction always produced small Pt particles evenly distributed over the support (Fig. 12a). When Pt which had only partially reacted with chlorine, evident from the observation of residual platinum

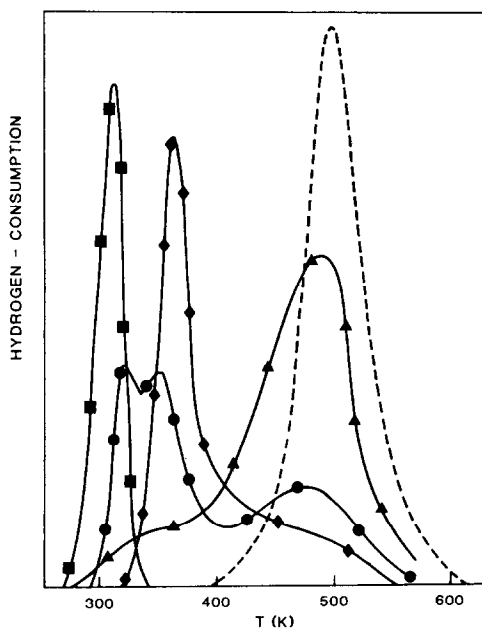


FIG. 9. Temperature-programmed reduction (TPR) profiles for Pt/SiO_2 treated in 10% Cl_2 in N_2 at $T_r = 320$ K (■), $T_r = 420$ K (▲), $T_r = 470$ K (●), $T_r = 570$ K (◆), and for 2.5% $\text{Pt}/\text{Al}_2\text{O}_3$ treated in 0.2–100% Cl_2 in N_2 at $320 < T_r < 700$ K (---). Sample sizes: 0.15 g for Pt/SiO_2 , 0.1 g for $\text{Pt}/\text{Al}_2\text{O}_3$.

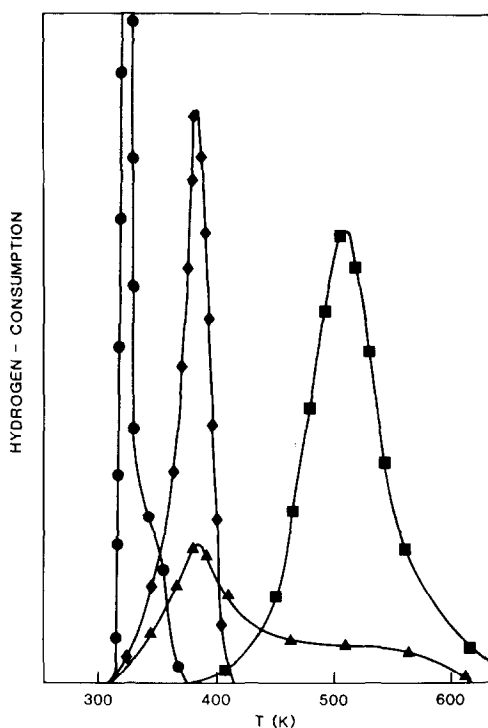


FIG. 10. Temperature-programmed reduction profiles. $\text{PtCl}_2 + \text{SiO}_2$ (\blacklozenge), $\text{PtCl}_2 + \text{SiO}_2$ —10% Cl_2 in N_2 , 670 K (\blacktriangle), $\text{PtCl}_2 + \text{Al}_2\text{O}_3$ (\bullet), $\text{PtCl}_2 + \text{Al}_2\text{O}_3$ —10% Cl_2 in N_2 , 670 K (\blacksquare). Sample size: 0.08 g.

particles by XRD and TEM, was reduced, the newly formed small Pt particles were also evenly spread over the support when

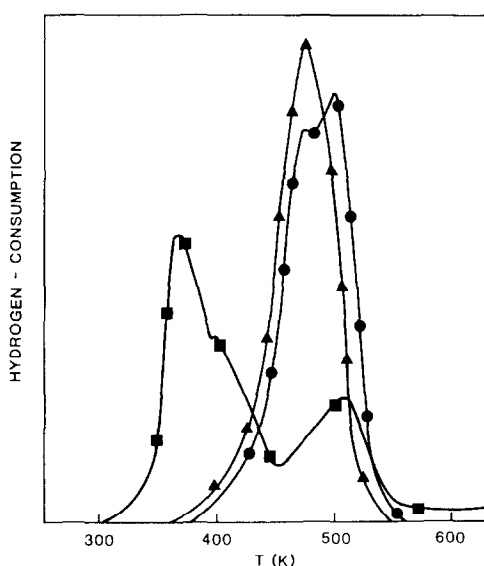


FIG. 11. Temperature-programmed reduction profiles of Pt/SiO_2 treated in streams containing $>25\%$ Cl_2 at $T_r = 470$ K (\blacktriangle), $T_r = 570$ K (\bullet), $T_r = 620$ K (\blacksquare). Sample size: 0.15 g.

T_r was above 470 K. When T_r was below 470 K, however, higher concentrations of newly formed small Pt particles close to remnants of large original Pt particles were observed after reduction (Fig. 12b). That reduction of Pt(IV) chloride which is formed exclusively on $\gamma\text{-Al}_2\text{O}_3$ invariably produced small Pt particles was further

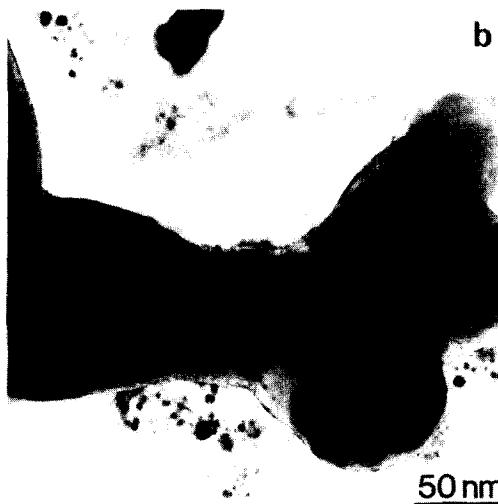
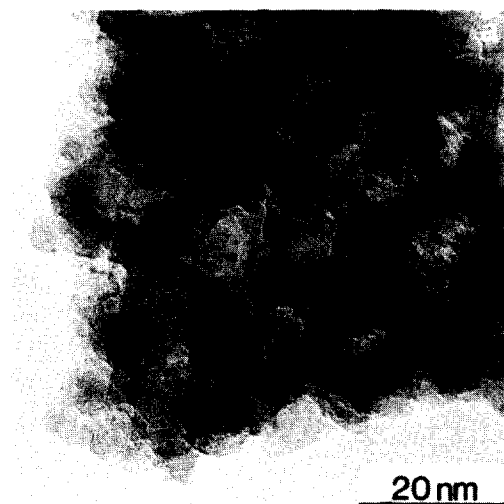


FIG. 12. Transmission electron micrographs of Pt on Al_2O_3 reacted with chlorine at 670 K followed by TPR (a), and at 520 K followed by TPR (b).

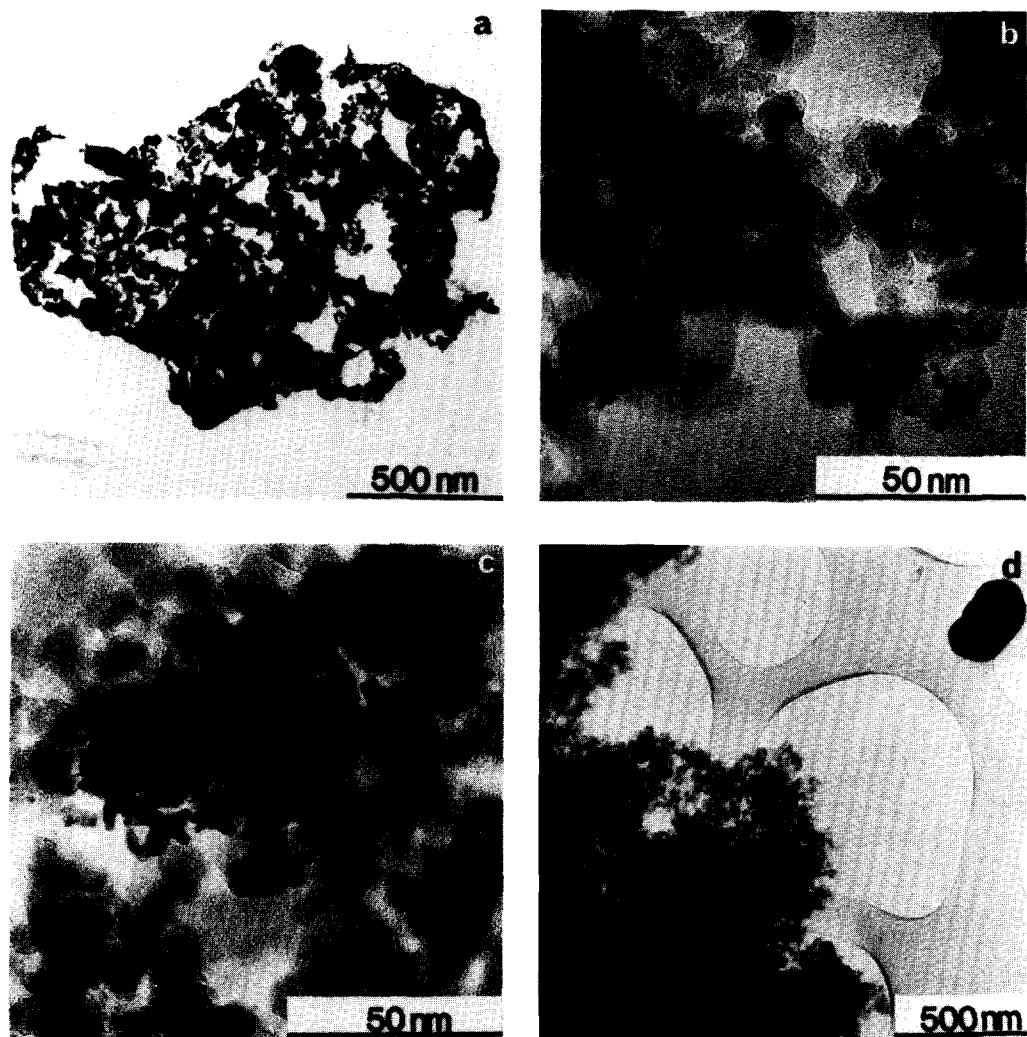


FIG. 13. TEM images of crystalline platinum chlorides on SiO_2 reduced below 520 K (a, b, c) and above 670 K (d).

confirmed with XRD traces where Pt peaks were always very broad.

Pt/SiO₂. The regular crystals of PtCl_2 , PtCl_3 , and PtCl_4 formed at certain values of T_r and Cl_2 concentrations on this substrate changed on reduction at temperatures < 570 K into contiguous aggregates of smaller Pt crystals while preserving the overall original shapes of the chloride crystals (e.g., see Fig. 13a). The web-like tangles and networks of Pt(II) chloride formed in 10% Cl_2 at $T_r < 400$ K converted into similar aggre-

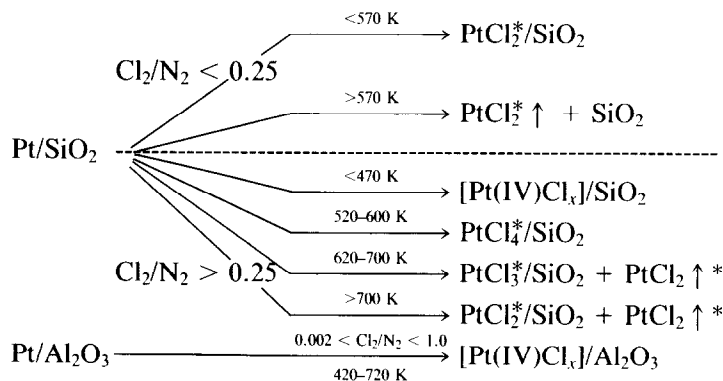
gates of Pt crystals when the reduction temperature was below 470 K (Fig. 13c). Higher temperatures (up to 770 K during TPR) caused the Pt to sinter and agglomerate into large crystals (Fig. 13d). Similarly to the situation on $\gamma\text{-Al}_2\text{O}_3$, noncrystalline Pt(IV) chloride, which was present to some extent under most conditions and which was the predominant product after chlorination at ≥ 470 K in treatment streams containing $\leq 25\%$ Cl_2 , was always converted into small Pt metal particles.

DISCUSSION

Reaction of Supported Platinum with Chlorine

Platinum supported on silica or alumina reacted readily with chlorine and complete conversion of the metal to the chlorides occurred at temperatures $T_r > 330$ K. In contrast Schäfer *et al.* (7) who studied the attack of chlorine on platinum powder in a static thermal gradient system reported that the buildup of chloride layers around platinum particles strongly inhibited the reaction at lower temperatures and that extensive conversion could only be achieved when aluminum halides (Al_2X_6) were added as "transport media." In a flow system, as used in this study, no inhibition did occur even at the lowest temperatures. Substantial chloride layers enveloping metal parti-

cles were never observed by TEM and the marked differences in the spatial distribution of products compared to the distribution of the originating metal particles indicated extensive vapor phase transport of the formed chlorides under flow conditions. The support material had no marked influence on the reaction rates. This was not surprising for Pt/SiO_2 and 2.5% $\text{Pt}/\text{Al}_2\text{O}_3$ considering that on both substrates platinum particles were far too large to exhibit a significant interaction with the substrate, but the smaller Pt particles (3 nm) present in 2.0% $\text{Pt}/\text{Al}_2\text{O}_3$ also were converted to platinum chlorides in similar time scales (see Table I). However, different end products result from the reaction of chlorine with platinum on SiO_2 and Al_2O_3 . As shown in the following scheme (where \uparrow indicates substantial



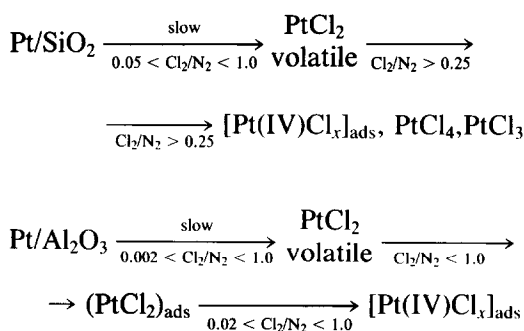
losses of products from the support and * indicates crystalline products) on silica crystalline platinum chlorides are produced under most reaction conditions. A noncrystalline product, which has been designated on the basis of its uv-vis spectrum as a $[\text{Pt(IV)Cl}_x]\text{--SiO}_2$ surface complex was formed at $T_r \approx 470$ K and $\text{Cl}_2/\text{N}_2 > 0.25$, but occurred only as minor product at low chlorine pressures. On $\gamma\text{-Al}_2\text{O}_3$, in contrast, the platinum metal is under all conditions converted exclusively into noncrystalline surface complex which was similarly desig-

nated as $[\text{Pt(IV)Cl}_x]\text{--Al}_2\text{O}_3$ on the basis of a comparison of its uv-vis spectrum with that obtained when $\gamma\text{-Al}_2\text{O}_3$ was impregnated with H_2PtCl_6 .

At the temperatures of the present experiments attack of chlorine on bulk platinum has been shown to produce initially highly volatile $\beta\text{-PtCl}_2$ (5, 7, 8). Since the Pt particles on both substrates and in particular on alumina are rather large to be influenced by metal-support interactions, we believe that it is justified to assume that PtCl_2 is the primary product from the reaction of chlorine

with Pt supported on silica and alumina. Although on the latter PtCl_2 could never be detected by TEM or XRD, its presence was indicated by the observation of a small TPR peak at 280 K when Pt on alumina had been reacted with chlorine at 470 K for only 2 h and which still showed the presence of metal particles by XRD and TEM. The reduction temperature, about 40 K lower than that observed when PtCl_2 was physically mixed with $\gamma\text{-Al}_2\text{O}_3$, was consistent with a platinum chloride in intimate contact with the metal, and the area under the TPR peak is consistent (assuming a composition of PtCl_2) with the platinum particles being covered with a few PtCl_2 layers.

The absence of substantial chloride layers around metal particles together with the observation that in such partially chlorinated catalysts Pt is mainly present as Pt(0) and Pt(4+) is indicative of a fast transport step as well as further chlorination reaction of PtCl_2 on alumina surfaces. PtCl_2 is not only the initial reaction product on both substrates but its formation seems to be the slowest step in the reaction scheme outlined below, which would explain the similar reaction rates observed on both substrates.



Those reaction models are further supported by the observations that when PtCl_2 mixed with both substrates was heated in Cl_2/N_2 streams containing 10% Cl_2 , on alumina complete redispersion of the chloride and conversion to a Pt(IV) compound was achieved at 520 K after only 0.5 h, while on silica no changes could be observed at

those temperatures and at higher temperatures PtCl_2 was lost from the support.

Oxidation of Pt^{2+} to Pt^{4+} by chlorine seems to be more readily accomplished on the support than it is in the gas phase. This is expected since adsorbing the chlorine on the substrate will lead to increased interaction with the PtCl_2 . If one compares the two substrates it is seen that on $\gamma\text{-Al}_2\text{O}_3$ the $[\text{Pt(IV)Cl}_x]$ surface complex formed exclusively over the whole range of conditions (470–670 K, % Cl_2 0.2–100) while on SiO_2 it formed in small amounts generally at low temperature but appeared exclusively only at 470 K provided the % Cl_2 was high (25–100). Thus it seems that on $\gamma\text{-Al}_2\text{O}_3$, chlorine not only readily facilitates the formation of a $[\text{Pt(IV)Cl}_x]$ surface complex but also greatly enhances its stability while on SiO_2 the influence of chlorine in this respect is much less pronounced. This observation is in agreement with the chemical nature of the surfaces involved. Platinum halide complexes exhibit a strongly anionic character and are therefore expected to interact more readily with $\gamma\text{-Al}_2\text{O}_3$, which in acid medium has been shown to adsorb anions, than with a hydrated SiO_2 surface, which has been observed to be a cation adsorber, albeit a very weak one. That $\gamma\text{-Al}_2\text{O}_3$ is more favorable than SiO_2 as a substrate for the oxidation of halide complexes with chlorine has also been observed for other platinum metals. For example, Kozlov *et al.* (9) found with PdCl_2 that in the presence of excess chloride ions, anionic complexes of higher oxidation state were formed on alumina and magnesia but not on silica.

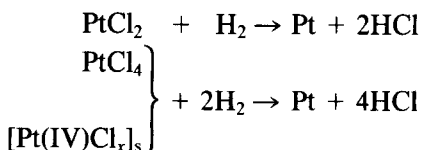
Differences in the behavior of $\gamma\text{-Al}_2\text{O}_3$ and SiO_2 similar to those observed here have also often been noted during the manufacture of catalysts. When platinum metal particles are produced on the two substrates by impregnating them with solutions containing H_2PtCl_6 , the anion PtCl_6^{2-} is readily adsorbed on $\gamma\text{-Al}_2\text{O}_3$, but it is taken up onto the SiO_2 only to a slight extent. Furthermore, TPR experiments (10) have shown that on SiO_2 the platinum in the an-

ion is readily reduced to the (2⁺) state by calcination at temperatures as low as 570 K (formation of PtCl₂), whereas on γ-Al₂O₃, in contrast platinum remains in the (4⁺) state even if calcined at temperatures as high as 770 K.

The mechanism of the interaction of aqueous solutions of H₂PtCl₆ with Al₂O₃ surfaces has been interpreted as either (i) an acid attack on the alumina surface with Al³⁺ ions going into solution and readsorption of these ions together with PtCl₆²⁻ to form surface complexes (11, 12) or (ii) a ligand displacement reaction, formulated as $ML_a^{n-} + O-Al- \rightleftharpoons ML_{a-1} \dots O-Al + L$, between the anionic chloride complex and the alumina surface (13). We believe that under the conditions of the present experiments (absence of aqueous phase, chlorinated substrates) ligand displacement reactions are more likely. However, in any case, on SiO₂ the bonds between the complex and the surface are obviously weak, since no surface complex is observed at any chloride concentration above 470 K. It is thus unlikely that PtCl₄ and PtCl₃ observed on SiO₂ are decomposition products of the surface complex, and the appearance of large crystals of those compounds rather suggests that they originate from a further reaction of chlorine with initially formed PtCl₂.

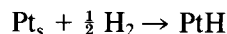
Reduction of Platinum Chloride Phases

The platinum chlorides formed by chlorination of Pt/SiO₂ and Pt/Al₂O₃ catalysts, reduce according to the schemes



and can be distinguished by TPR. PtCl₂ physically mixed with the two substrates or dispersed on the substrates gives rise to TPR maxima in the range 310 to 360 K. PtCl₄, [Pt(IV)Cl_x]_s reduce in the temperature range 450 to 550 K and TPR profiles of

PtCl₃ showed a large maximum at 370 K and a smaller one at 500 K. The amounts of hydrogen consumed in the TPR experiments thus provide a quantitative measure of the oxidation state of platinum in the catalyst after chlorine treatment (cf. Table I). Adsorption of hydrogen on surface platinum atoms contributes



very little to the overall hydrogen consumption during a TPR experiment, since (i) whenever highly dispersed catalysts (large platinum surface area) are obtained, reduction takes place above 470 K, a temperature where the hydrogen coverage of the surface is already significantly reduced, and (ii) when the reduction occurs at lower temperatures (crystalline PtCl₂) catalyst of low platinum surface areas result.

Redispersion of Platinum

A comparison of the average platinum particle sizes of the catalysts before and after chlorine treatment (Table I), shows that redispersion of the metal—decrease in particle size—was associated with the formation of a [Pt(IV)Cl_x]_s surface complex. Whenever crystalline chlorides were present as major products contiguous aggregates of smaller platinum crystals formed on reduction at lower temperatures (Fig. 13) or large platinum crystals at high reduction temperatures (Fig. 13d) and in general those particles were larger than the ones present before chlorine treatment. Platinum on Al₂O₃ was shown to convert exclusively to the [Pt(IV)Cl_x]_s surface complex at all treatment conditions and homogeneously distributed small metal particles are generally observed after reduction of the chlorine-treated catalyst. Birke *et al.* (14), who studied the effects of chlorine treatment on Pt–Al₂O₃ reforming catalysts reported in agreement with our study that an increase in platinum dispersion is intimately connected with the presence of a chloride phase containing platinum in the 4+ oxidation state, but their findings that

such compounds form only in chlorine-oxygen (air) mixtures or by further treatment of the chlorinated catalyst in oxygen are difficult to reconcile with the present results. The discrepancies may originate from (i) Birke *et al.* used a treatment gas with lower chlorine concentration (0.15% compared to our lowest concentration of 0.2%); (ii) most of Birke's experiments were carried out above 670 K whereas our study was done in the temperature range 470 to 670 K.

Furthermore, Birke *et al.* were unable to directly identify the Pt compound formed during the treatment and determined the Pt oxidation state by indirect methods, and a close examination of their data revealed that air treatment at temperatures in the range 700 to 850 K of a Pt/Al₂O₃ catalyst pretreated for 5 h in 0.15% Cl₂/N₂ at 723 K led to only insignificant improvements in the percentage of oxidized Pt present in the catalyst and in the metal dispersion of the subsequently reduced catalyst.

With Pt/SiO₂ redispersion was achieved only by treatment in gas streams containing >25% chlorine and at $T_r < 500$ K. Partial redispersion was possible at lower chlorine concentrations in the temperature range 350 to 450 K, but besides small metal particles large platinum aggregates, originally from the reduction of Pt(II) chlorides, were also present.

CONCLUSIONS

Successful redispersion of platinum by chlorine treatment is achieved in a four-step process: (i) attack of platinum particles to form volatile β -PtCl₂; (ii) vapor phase transport of the chloride; (iii) adsorption of the PtCl₂ molecule; and (iv) further chlorination to form complex chlorides of Pt⁴⁺,

strongly bound to the surface. With Pt/Al₂O₃ the formation of anionic complexes of Pt(IV) is favored, due to the relatively strong interaction of such compounds with the alumina surface and an increase in metal dispersion is generally observed after chlorine treatment followed by reduction. The interaction of a Pt(IV) chloride complex with a silica surface is rather weak and redispersion requires (a) a high chlorine concentration (>25 vol%) in the treatment gas and (b) a reaction temperature < 500 K to prevent the decomposition of the surface complex to crystalline chloride.

REFERENCES

1. Sittig, M., "Handbook of Catalyst Manufacture," pp. 453-462. Noyes Data Corporation, Park Ridge, N.J., 1978.
2. Birke, P., Engels, S., Becker, K., and Neubauer, H. D., *Chem. Tech.* **31**, 473 (1979).
3. Delannay, F., Defosse, C., Delmon, B., Menon, P. G., and Froment, G. F., *Ind. Eng. Chem. Prod. Res. Dev.* **19**, 537 (1980).
4. Foger, K., and Jaeger, H., *J. Catal.* **67**, 252 (1981).
5. Degner, M., Holle, B., Kamm, J., Pilbrow, M. F., Thiele, G., Wagner, D., Weigl, W., and Woditsch, P., *Transition Met. Chem.* **1**, 41 (1975/76).
6. Pilbrow, M. F., *J. Chem. Soc. Chem. Commun.* 270 (1972).
7. Schäfer, H., Wiese, U., Brendel, C., and Nowitzki, J., *J. Less-Common Met.* **78**, 68 (1980).
8. Wiese, U., Schäfer, H. V., Schnering, H. G., Brendel, C., and Rinke, K., *Angew. Chem. Int. Ed.* **9**, 158 (1970).
9. Koslov, N. S., Kravchuk, L. S., Lazarev, M. Ya., Stremok, I. P., and Pavlovich, S. V., *Russ. J. Phys. Chem.* **46**, 741 (1972).
10. Jenkins, J. W., *Prepr. 6th Canad. Symp. Catal. Ottawa, 1979*, p. 21.
11. Santevesaria, E., Carra, S., and Adami, I., *Ind. Eng. Chem. Prod. Res. Dev.* **16**, 41 (1977).
12. Parkash, S., Chakrabarty, S. K., and Koanigawa, T., *Fuel Process. Technol.* **6**, 177 (1982).
13. Summers, J. C., and Ausen, S. A., *J. Catal.* **52**, 445 (1978).
14. Birke, P., Engels, S., Becker, K., and Neubauer, H. D., *Chem. Tech.* **32**, 253 (1980).